Unoccupied electronic states of 2D Si on Ag-$\sqrt{}$ 3-Si(111)

H Mrezguia, L Giovanelli, Y Ksari, A Akremi, J.-M Themlin

Unoccupied electronic states of 2D Si on Ag-$\sqrt{3}$-Si(111)

H. Mrezguia,[1,2] L. Giovanelli,[1] Y. Ksari,[1] A. Akremi,[2] and J.-M. Themlin[1]

[1] *Aix Marseille Univ, Univ Toulon, CNRS, IM2NP, Marseille, France*

[2] *Université de Carthage, Laboratoire de Physique des matériaux, LR01ES15: Structure et Propriétés, Faculté des Sciences de Bizerte, 7021 Jarzouna, Bizerte, Tunisia*

(Dated: February 16, 2021)

Optimizing substrate characterization to grow 2D Si layers on surfaces is a major issue towards the development of synthesis techniques of the promising silicene. We have used inverse photoemission spectroscopy (IPES) to study the electronic band structure of an ordered 2D Si layer on the $\sqrt{3}\times\sqrt{3}$ -Ag/Si(111) surface ($\sqrt{3}$-Ag). Exploiting the large upwards band bending of the $\sqrt{3}$-Ag substrate, we could investigate the evolution of the unoccupied surface and interface states in most of the Si band gap. In particular, the $k_{\|}$-dispersion of the $\sqrt{3}$-Ag free-electron-like S_1 surface state measured by IPES, is reported for the first time. Upon deposition of ∼1 ML Si on $\sqrt{3}$-Ag maintained at $\sim 200^{\circ}$C, the interface undergoes a metal-insulator transition with the complete disappearance of the S_1 state. The latter is replaced by a higher-lying state U_0 with a minimum at 1.0 eV above E_F. The origin of this new state is discussed in terms of various Si 2D structures including silicene.

INTRODUCTION

Due to the lack of a 2D allotrope form of Si and at variance with graphene, silicene does not exist in a self-suspended form [1]. As a consequence a great deal of effort was recently devoted in the search of a suitable support for its growth through heteroepitaxy [2–5]. On the other hand, a benefit with respect to graphene is given to silicene for its tendency to rehybridization and consequent buckling when forced in 2D [3]. This, together with a higher spin-orbit coupling, confers to silicene a larger electronic energy gap which increases its appeal towards the realization of a quantum spin Hall topological insulator [6]. Several studies have further revealed that buckling can be modified through the interaction with the substrate [7]. This may in principle increase the electronic gap but the interactions should be handled with care since drawbacks such hybrid interface states with undesired metallic character can appear [8].

Since the choice of a suitable substrate with adequate properties is crucial for heteroepitaxy, different ways of growth were explored for silicene synthesis [9]. Intercalation with rare-earth atoms [10] and segregation into a ZrB_2 buffer layer [11, 12] both use Si(111) as a common substrate whereas a buffer layer of suitable atoms opens ways for tuning the epitaxy process [13, 14]. In this context, Ag(111) is certainly the most explored substrate since it combines the right reactivity with a good lattice mismatch allowing several phases of silicene to develop [15–18]. Moreover, the possible presence of Dirac cones in the electronic structure has spurred a large number of studies and lively debate [19–26].

Ag(111) was also pointed out as a preferred substrate for multilayer growth [9, 27–29]. Because of its intrinsic interest in technological applications, the quest for multilayer silicene stimulated considerable scientific interest and controversy in the results interpretation. Namely the presence of Ag at the surface was detected in some cases [30, 31] and its role as a surfactant for diamond-like Si multilayer growth was highlighted [32, 33]. At the same time the stringent role played by quality of the first adsorbed Si layer for further multilayer growth [9] as well as the role played by the substrate temperature [28] was emphasized.

Following the promising results obtained on Ag(111), the $\sqrt{3}\times\sqrt{3}$ -Ag/Si(111) ($\sqrt{3}$-Ag for short) was recently introduced as a new candidate for silicene growth [34]. The $\sqrt{3}$-Ag surface is very well known in surface science and was considered as an ideal playground for metal-semiconductor interface studies [35–38]. The Ag adsorption saturates the Si(111) dangling bonds, resulting in a complex interface atomic arrangement eventually rationalized in a inequivalent triangle model [36, 37]. Due to the confinement of the Ag *sp* electrons at the interface with underlying Si, the $\sqrt{3}\times\sqrt{3}$ surface is known to be less reactive with respect to foreign atom adsorption as compared to Ag(111) [39]. This substrate proved to be well suited to the growth of well-ordered multilayer silicene whose structure was characterized in a multi-technique approach including *ab initio* calculations [34]. As far as the interface with Si is concerned, this is supposed to play an important role for the growth of further layers. Calculations suggested a mild interaction through Si-Ag bonding resulting in a freestanding (FS) structure with increased buckling. As in the case of Ag(111), the substrate temperature was shown to play a fundamental role for multilayer growth. Subsequently, an electronic structure investigation was also performed on the multilayer silicene grown on $\sqrt{3}$-Ag with the help of DFT calculations [40].

The perspective of a new substrate as a support for high-quality silicene grown by molecular beam epitaxy calls for further investigation. In the present study the focus is put on the seeding layer for multilayer growth, namely single layer silicene on $\sqrt{3}$-Ag , from the electronic structure (unoccupied states) point-of-view. The

approach consisted in following in detail the protocol employed in previous studies [34] for the preparation of a single layer of Si on $\sqrt{3}$-Ag and to assess the surface quality through a comparison of structural and elemental results by low-energy electron diffraction (LEED) and Auger electron spectroscopy (AES). The unoccupied states were then probed by k-resolved inverse photoemission spectroscopy (KRIPES). Starting with the pristine $\sqrt{3}$-Ag surface, a proper Ag adatom concentration allowed to address the well known S_1 surface state whose angular dispersion in the empty states was measured by KRIPES for the first time. Subsequently, the evolution of the electronic structure of the Si interface occurring upon Si deposition at 200 °C was measured and elucidated through a comparative study of possible scenarios. Namely, KRIPES of Si single layer shows the quenching of the $\sqrt{3}$-Ag surface state and the appearance of a new feature in the Si(111) bulk-projected band gap. Such feature can be assigned to empty states originating from a single layer of silicene interacting with the $\sqrt{3}$-Ag substrate.

EXPERIMENT

The experiments were carried out in a ultra-high vacuum (UHV) system composed of a preparation chamber and an analysis chamber with a base pressure below $10^{-10}mbar$. The preparation chamber consisted of an electron bombardment heating system, an electron-beam metal evaporator for Ag deposition and a Si evaporator composed of a Si wafer lying at 4-5 cm distance and heated by direct current (21 W power).

The sample annealing was performed through radiative heating (up to 600 °C) and electron bombardment (higher temperatures) from a tungsten filament close to the back-side of the sample. The sample temperature was monitored by a pyrometer in the high temperature range while a direct calibration with a thermocouple was performed prior the experiment for the low-temperature measurements. This procedure was particularly important in order to obtain the right temperature for the silicene formation. The calibration was performed with the Si wafer kept at sublimation temperature since we noticed that during sublimation, the latter brought a significant fraction of the total power received by the sample.

The analysis chamber is equipped with a LEED apparatus also serving as a retarding field analyzer for AES and an inverse photoemission spectroscopy (IPES) system. The process of inverse photoemission involves the emission of photons when a collimated incident electron beam strikes the surface of a solid sample. Electrons enter the sample through coupling to the unoccupied electronic bulk or surface states at the incident electron energy E_i. Some of these electrons drop to lower-energy unoccupied states above the Fermi level (E_F) through the emission of a photon. The radiative transitions detected in IPES involve unoccupied electronic states with energies E_i and E_f (wrt E_F), linked by $E_i - h\nu_0 = E_f$. The IPE spectra presented here are obtained in the so-called isochromat mode, where photons of a fixed energy $h\nu_0$ (in this case around 9.7 eV) are collected by a band-pass detector while sweeping the incident-electron beam energy. The energy and angular resolution are, respectively, 0.6 eV and 0.1 $\mathring{A}^{-1}$ [41]. Furthermore, owing to the conservation of the parallel component of the electron wave-vector when it crosses the surface barrier, the optical transitions can be located along selected rods of the reciprocal space, perpendicular to the surface Brillouin zone, making IPE a $k_{\|}$-resolved spectroscopy (KRIPES). The KRIPES spectra are obtained by rotating the sample around an axis parallel to the surface plane and perpendicular to the fixed electron beam. Since the sample is carefully oriented using the LEED pattern, it is thus possible to follow the sample unoccupied band structure along high-symmetry directions of the surface Brillouin zone.

The sample preparation consisted in three steps. After five hours outgassing of a freshly introduced sample ($5\times15\ mm^2$ cut from a n-doped Si(111) wafer of 0.13-0.37 Ωm resistivity), the production of a (7×7)–reconstructed surface was achieved by several flash annealings up to 1050 °C in the $10^{-10}mbar$ range followed by a slow (-20 °C/min) decrease down to 860 °C. A sharp 7×7 LEED pattern and, more importantly, an intense peak in the IPE spectrum attributed to an adatom-derived surface state are fingerprints of the good surface quality. Subsequently the $\sqrt{3}$-Ag was produced by depositing one monolayer of Ag onto the Si sample pre-heated for 20 minutes and kept at 500 °C. The sample showed a sharp $\sqrt{3}\times\sqrt{3}$ LEED pattern and an IPE spectrum with metallic surface state [42]. Finally, the silicene layer was obtained by exposing for 60 minutes a freshly prepared $\sqrt{3}$-Ag surface kept at 200 °C (pre-heating 30 minutes) to the Si atom flux. The Si deposition time was adjusted so to obtain the same Auger spectrum reported in Ref. [34]. The resulting surface showed a $\sqrt{3} \times \sqrt{3}$ LEED pattern similar to the one obtained in those previous studies.

RESULTS

As stated in the introduction, particular attention was devoted in the present study to reproduce the experimental conditions reported in Ref. [34]. In Fig. 1 the AES spectra before (red) and after (blue) deposition of the Si single layer on $\sqrt{3}$-Ag are reported together with the corresponding LEED patterns. The two spectra are normalized to the Si-LVV peak to peak intensity and the inset of the Ag-MNN peak shows the small reduction expected for a single layer of Si on $\sqrt{3}$-Ag [34]. Due to the different apparatus used in the two experiments,

the ratio between the Si and Ag peaks for each sample is sensibly smaller than what observed previously. However, the relative reduction of the peak ratio upon Si deposition is very close, ensuring a suitable Si coverage in the monolayer range. The LEED pictures both display a $\sqrt{3}\times\sqrt{3}$ pattern due to the pristine $\sqrt{3}$-Ag substrate and the adsorbed Si adlayer (see the discussion below). As expected the latter has higher diffusive background due to the less ordered surface revealed by STM analysis [34].

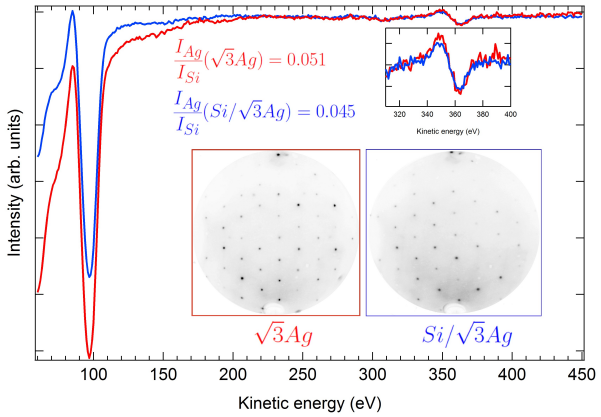

FIG. 1: (color online). Auger spectra (primary electron energy 1200 eV) and LEED patterns (primary electron energy 50 eV) of the pristine $\sqrt{3}$-Ag surface (red) and after the deposition of a single layer of Si (blue).

In Fig. 2 a set of IPE spectra as a function of incident angle along the $\overline{\Gamma}-\overline{M}_{\sqrt{3}}$ direction is presented together with a least-squares fit of the low-energy region. The normal incidence (NI) spectrum is also displayed in a wide energy range to discuss the different features representative of the $\sqrt{3}$-Ag surface. The highest energy peak around 4.6 eV has been attributed to a bulk direct transition to the Λ_3 unoccupied band along the $\Gamma-L$ line [42]. A second transition to a lower energy band of the same symmetry is present at around 3.2 eV as a shoulder of the largest peak and labeled Λ_1. Finally, the largest peak measured at 2.5 eV can be assigned to a direct transition occurring at the edge of the bulk-projected unoccupied band structure and observed close to NI thanks to a surface umklapp process through the Ag-($\sqrt{3}\times\sqrt{3}$) reciprocal lattice [42]. This bulk-related feature becomes visible thanks to the presence of the $\sqrt{3}$-Ag reconstruction. In the vicinity of the Fermi level a clear feature can be assigned to S_1, one of the three surface states of this surface [35]. It is a well documented free-electron parabola having Ag $5p_x$ and $5p_y$ components with a minimum located just above the valence band maximum [35, 43–45]. The parabola can be downward-shifted in energy upon adatom adsorption which has important effects in 2D surface transport [35]. Because the partially occupied S_1 state guarantees Fermi level pinning and hole accumulation layer, its occupation also tunes the upward band bending [43]. Its energy dispersion was studied in the occupied states by angle-resolved photoemission [46] and in the unoccupied states with scanning tunnelling spectroscopy [47]. In the present study, the substrate temperature in preparing the $\sqrt{3}$-Ag surface allowed to keep the adatom concentration at low values which ensured a strong band bending [63]. As a result, a larger energy range is available to follow the S_1 dispersion within the energy gap. A previous IPE study first revealed its presence and its metallic character [42] but did not address the unoccupied band dispersion because of the presence of the nearby bulk peaks which, in that case, appeared at lower energy.

The angular dispersion of S_1 and of the umklapp feature is displayed as a function of $k_{||}$ in the up-right inset of Fig. 2. The upward dispersion observed for the umklapp feature suggests that it should come from a critical point along a rod passing through $\overline{K}_{1\times1}$ [42] in which the band structure has a local minimum. Concerning the S_1 feature, the fitting functions used as a model are highlighted for each spectrum in the up-left inset. Due to the limited angular resolution, a clear take-off at the Fermi level is observed up to an electron incidence angle of 12.5 °. This is modeled by a gaussian times the Fermi-Dirac function plus an integral background [46]. At higher energies a simple gaussian is used. A thick mark is set at the gaussian position above each S_1 peak also in the main panel as a guide to the eye.

At variance with the bulk feature, S_1 displays a steep dispersion with an almost linear behavior up to 0.28 $\mathring{A}^{-1}$ where the presence of the bulk feature renders the fitting procedure less reliable. The free-electron character of S_1 is well-known and a least-squares regression to a parabola can give insight on the carrier effective mass [46]. In the present case, due to the limited energy and angular resolution inherent to IPE such procedure would be pointless. Nevertheless the data indicate that the Fermi wave vector should be smaller than approximately 0.05 $\mathring{A}^{-1}$ in agreement with ARPES measurements [35, 48] for a low concentration of Si adatoms.

The presence of the S_1 surface state testifies of a good surface quality, a prerequisite for the successful growth of the silicene layer [34]. Following the procedure detailed in the Experiment section, a single layer of Si was deposited on a freshly-prepared $\sqrt{3}$-Ag surface kept at 200 °C. The KRIPES taken on the Si/$\sqrt{3}$-Ag surface is displayed in Fig. 3 together with the comparison, at the bottom of the figure, of the spectra taken before and after Si deposition. Such comparison allows to appreciate two changes. The first concerns the bulk peaks: an attenuation due to the presence of the Si overlayer and a shift to lower energies, due to the disruption of the S_1 surface state which no more pins the Fermi level and causes a reduction of the band bending. On the other hand a substantial change in the spectral line shape occurs within the bulk band gap (see also the low-energy region of the magnified spectra

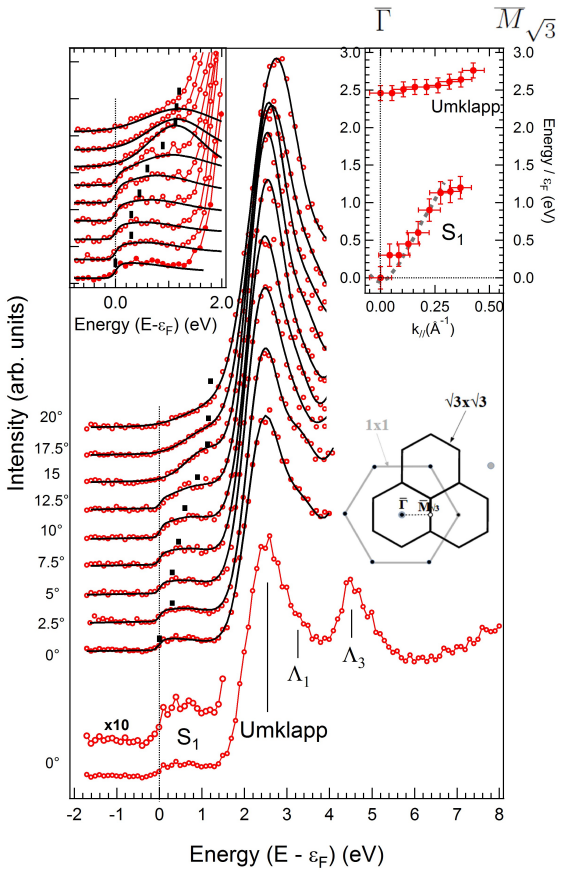

FIG. 2: (color online). KRIPES spectra of the $\sqrt{3}$-Ag surface. Central panel: the bottom wide range spectrum is taken at normal incidence ($\Theta = 0°$), then, from bottom to top the incidence angle is increased to explore the $\overline{\Gamma} - \overline{M}_{\sqrt{3}}$ direction. The spectra are displayed in a shorter energy range and are accompanied by a least-squares fit (blue lines). The top-left panel displays a blow-up close to the Fermi level together with a fitting function (see text for details). In the top-right panel the dispersion of two of the states detected by KRIPES is displayed between $\overline{\Gamma}$ and $\overline{M}_{\sqrt{3}}$. A computed dispersion of the S_1 state taken from Ref.[49] is displayed as dashed line. The unreconstructed Si(111)-1×1 and $\sqrt{3} \times \sqrt{3}$ surface reciprocal lattices and surface Brillouin zones are also depicted as grey (resp. black) points and lines.

at the bottom of Fig. 3). Here the "metallic" S_1 band is replaced by a higher energy feature U_0 centered at about 1 eV with a fading intensity at the Fermi level. Its angular dependence is highlighted in the up-left inset where the fitting is also reported. A simple gaussian is used here due to the vanishing contribution at the Fermi level. The dispersion is very small in the angular region where for the $\sqrt{3}$-Ag surface it was the most important. This can be clearly seen in the top-right inset where the energy dispersion obtained from the fitting is compared to S_1 (shaded markers). Comparatively, the bulk band structure has not changed substantially upon Si deposition : its features are reduced in intensity but maintains the same dispersion. It is important to notice that the presence of the U_0 feature is very sensitive to the substrate temperature during Si deposition. This can be seen in Fig. S1 of Supplementary materialwhere in NI spectra taken after depositing 1 ML Si at substrate temperature higher or lower than 200 °C the disappearance of S_1 is not accompanied by the presence of U_0.

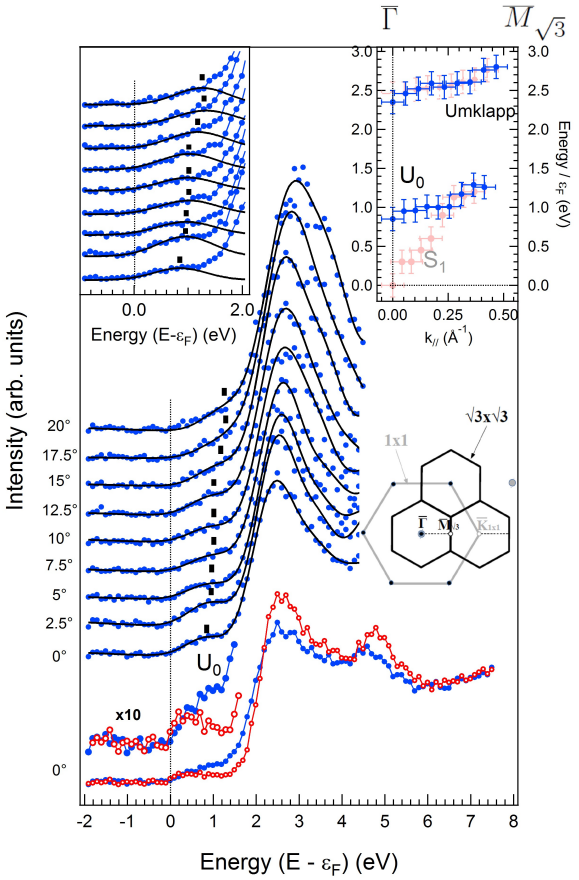

FIG. 3: (color online). KRIPES spectra of the Si layer deposited on $\sqrt{3}$-Ag surface, for increasing incidence angle θ along the $\overline{\Gamma} - \overline{M}_{\sqrt{3}}$ direction. At the bottom the NI spectrum before Si deposition (red open circles) is also reported for comparison with the normal incidence IPE spectrum after Si deposition (blue filled circles). The upper panels are like in Fig. 2 and the dispersion of the S_1 state (pink shaded circles) is reported in the top-right panel for comparison. The unreconstructed Si(111)-1×1 and $\sqrt{3} \times \sqrt{3}$ surface Brillouin zones are also depicted to highlight the coincidence between $\overline{K}_{1\times1}$ and $\overline{\Gamma}_{\sqrt{3}\times\sqrt{3}}$.

DISCUSSION

As stated in the introduction, silicene can only be found on a solid surface acting as a support for its growth. Structural order and coherence of the 2D honeycomb network strongly depends on the quality of the chosen

substrate. Moreover, DFT calculations suggested that silicene may be present in different metastable phases. As a consequence, the growth conditions (including Si atom flux and substrate temperature) are particularly important. The approach used in the present paper is to strictly follow a former multi-technique study [34] in which single layer silicene formation was assessed on the $\sqrt{3}$-Ag surface and to use some of the structural and elemental techniques employed in that study as characterization benchmarks. In the following we discuss the new experimental facts resulting from coupling such procedure with KRIPES results in terms of the possible presence of a silicene layer.

The good quality of the employed substrate is proved by the presence of a surface state whose dispersion in the unoccupied states was measured here for the first time by inverse photoemission. The substrate should then be suited to the growth of 2D Si layers and possibly to silicene. Before attempting to interpret our results in terms of silicene formation, it is important to sift through other scenarios that could fit our data. Summarizing the previous section, the adsorption of one monolayer of Si on $\sqrt{3}$-Ag kept at 200 °C resulted in a surface keeping a $\sqrt{3}\times\sqrt{3}$ LEED pattern. The electronic structure showed a new state in the gap (named U_0 in Fig. 3) with vanishing DOS at the Fermi level and a sensible flattening of the band bending.

In the perspective of a possible modification of the S_1 state after Si deposition, it is useful to recall previous studies on the behavior of the surface states of the $\sqrt{3}$-Ag surface upon adsorption of foreign species. In general, this surface is expected to be less reactive as compared to Ag(111) [39]. It is then not surprising that it allows the growth of ordered overlayers such as, for instance, organic architectures [50, 51] which are otherwise rarely observed on bare Si surfaces. When π-conjugated molecules are adsorbed the S_1 surface state is generally preserved, and the energy shift which is observed can be explained by charge transfer to or from the overlayer [52].

When exposed to more reactive species such as noble metal (Ag) or alkali (Na) adatoms, the situation is different. Although the structural elements of the $\sqrt{3}\times\sqrt{3}$ structure are preserved underneath, the adsorption of adatoms on Ag trimers induces a $\sqrt{21}\times\sqrt{21}$ reconstruction, strongly affecting the electronic structure [45]. The S_1 state receives charge from partially ionized adatoms and the Fermi level is thus raised by tenths of eV. At the same time, due to the interaction potential of charged donors, the backfolding of S_1 adds to this band a new surface state separated from S_1 by an energy gap. This new state, reminiscent of S_1, displays a strong angular dispersion in ARPES [53].

In the case of Si adsorption the above scenarios are not expected to occur. The main ingredients for a simple evolution of the $\sqrt{3}$-Ag structure as depicted above are missing, most importantly the presence of a strongly dispersing band. Moreover, there is no sign of evolution in the LEED pattern similar to the typical $\sqrt{21}\times\sqrt{21}$, probably because the adsorption of Si promotes strong covalent bonding with Ag. As a consequence the Si atoms are not expected to have enough surface mobility to develop long-range periodic perturbations as in the case of noble or alkali metal adsorption. The $\sqrt{3}$-Ag structure is expected to be destroyed by Si adsorption and the S_1 state to vanish rather than to evolve in a gapped nearly free-electron surface state which should show a parabolic dispersion not observed here.

Another explanation should take into account a possible segregation of the interface Ag atoms above the deposited Si layer. Ag is known to segregate from multilayer [32, 33] and monolayer [54] Si when the actual substrate is Ag(111). This has stimulated a debate on the origin of spectroscopic features initially attributed to Dirac cones and on the actual role of growth temperature of genuine silicene multilayers [19–26]. Later on, Ag atoms were found to segregate with a surfactant role for the growth of Si layers even when the $\sqrt{3}$-Ag surface was employed as a support [55]. This was inferred from ARPES measurements showing dispersion patterns reminiscent of the $\sqrt{3}$-Ag before Si deposition, just as it was found for Si multilayers on Ag(111) [56]. However, Ag atoms need to overcome an activation barrier to allow segregation. It was argued that if the substrate temperature is kept in a narrow window around 200 °C a multilayer silicene growth occurs [34]. Our results seem to confirm this scenario, at least in the single layer regime, since no S_1-derived dispersing features are observed. The fact that in the present case the temperature was kept around 200 °C probably prevents the Ag atom to leave their original sites.

Let us then examine the possibility of the formation of a 2D Si layer displaying the $\sqrt{3}\times\sqrt{3}$ structure. A $\sqrt{3}\times\sqrt{3}$ *without* silicene has been reported in the past as extended domains on the Si(111) surface [57]. Different models were proposed among which a buckled $\sqrt{3}\times\sqrt{3}$ structure was shown to be energetically separated from the stable 2×1 π-bonded chain reconstruction [58]. This $\sqrt{3}\times\sqrt{3}$ -Si(111) metastable phase is vacancy-stabilized and experimentally it was observed after flash annealing at 1000 °C a surface previously damaged by ion sputtering. If on one side one can consider such a picture with the Si adsorption forcing the Ag atoms out from their original sites, the promotion of extended regions of $\sqrt{3}\times\sqrt{3}$ -Si would need a much higher annealing temperatures than that employed here [57, 58]. Moreover, the expected electronic structure should be metallic [58], which is not what we observe by IPES. Another case in which $\sqrt{3}\times\sqrt{3}$ was observed on bare Si(111) surfaces was more recently found by desorbing Tl single layer by thermal annealing at 550 °C [59], which is too high to be considered as a plausible scenario here. Finally, a recent study reported on a $\sqrt{3}\times\sqrt{3}$ -Si(111) obtained by mul-

tilayer Si growth on Ag(111). In that case a new surface state (not related to Ag atoms) was found to develop [60]. Its strongly dispersing character does not correspond to what found here and can then be excluded to be at the origin of the U_0 feature.

More realistically, the presence of an extended 2D Si network referred to as silicene, preserving the $\sqrt{3} \times \sqrt{3}$ structure of the Ag/Si(111) substrate, can be considered. Such structure was measured by De Padova *et al.* [34] on $\sqrt{3}$-Ag and it is thus likely to occur in the present study where the same experimental conditions have been reproduced with care. In this former work, the silicene signature was measured in the filled states (ARPES) in the multilayer case, and the experimental features could be addressed by comparison with DFT calculations of 4 ML of silicene on $\sqrt{3}$-Ag . In that case the interface with the substrate gave a minor contribution to the calculated band structure which is less useful here where only 1 ML is probed. Alternatively, one can refer to the single layer silicene band structure calculations performed for adsorption on Ag(111), where similar Si-Ag interactions are expected.

Starting from the self-supported case, one of the main characteristics of the free-standing silicene is to preserve its honeycomb structure despite the buckling. This allows the presence of Dirac cones at the K points of the 2D Brillouin zone even though, as compared to graphene, the hybridization deviates from simple sp^2 through a π–σ rehybridization [61]. When adsorbed on the Ag(111) surface, the interface interaction increases the buckling in a site-dependent fashion, thus breaking the symmetry within the honeycomb lattice and opening a gap at K points. Moreover, the Si-Ag interaction results in the development of hybrid interface states. Whether or not Dirac cones do result from the interface electronic structure rearrangement is still a matter of debate [23, 26] but the original band structure is strongly affected. This was visualized by first-principle calculations by the unfolding of the interface electronic structure [24, 62]. It appears that the Fermi level shifts upwards and, within the hybrid electronic states, a remnant of the FS silicene electronic structure displays a large gap at Γ whereas, as far as low-energy states are concerned, they are concentrated at zone boundaries ($\overline{K}$ and $\overline{M}$ points of the (1× 1) silicene Brillouin zone) [62].

At first sight such electronic structure may seem at odds with our KRIPES spectra showing low-energy features in the gap around normal incidence (NI). Nevertheless, a more accurate analysis of the inverse photoemission process reveals that not only Si-derived interface states should be expected around NI but that these may represent the signature of the 2D Si lattice referred to as silicene. Since the silicene $\overline{K}$ point coincides with the $\overline{\Gamma}$ point of the $\sqrt{3} \times \sqrt{3}$ reconstruction (see the inset of the surface Brillouin zones [64] in Fig. 3), transitions occurring at $\overline{K}$ (about 1.1 Å^{-1} away from $\overline{\Gamma}(1 \times 1)$) can be back-folded to NI. The U_0 state detected after Si deposition may then be tentatively ascribed to surface states localized near the $\overline{K}$ point. For slightly higher wave vector values and lower energies, a Si-Ag hybrid band disperses through the Fermi level [62] in the calculations.

Using the results obtained theoretically for silicene/Ag(111) may seem a stretch. Although new band structure calculations are highly desirable, the use of silicene/Ag(111) as model system for KRIPES interpretation on $\sqrt{3}$-Ag is somehow justified by the fact that structural data calculated for silicene/$\sqrt{3}$-Ag [34] show similar values for the silicene-substrate distance ($\sim$ 2.2 Å as compared to 2.13 Å) and buckling (Δz=0.69 Å and 0.78 Å , respectively) as compared to silicene/Ag(111).

CONCLUSIONS

In conclusion the unoccupied part of the electronic band structure of a 2D Si layer on the $\sqrt{3} \times \sqrt{3}$ -Ag/Si(111) surface ($\sqrt{3}$-Ag) was studied by inverse photoemission spectroscopy. Taking advantage of the Fermi level pinning at the top of the valence band, the Si substrate high upwards band bending allows to explore the unoccupied states within the whole Si band gap. The $k_{\parallel}$-dispersion of the $\sqrt{3}$-Ag S_1 surface state measured in KRIPES was reported for the first time.

Upon deposition of $\sim$1ML Si at 200 °C, the interface undergoes a metal-insulator transition with the complete disappearance of the S_1 state, replaced by a higher-lying state U_0 centered at around 1.0 eV above E_F. An interface state originating from a Si monolayer referred as silicene interacting with the $\sqrt{3} \times \sqrt{3}$ -Ag/Si(111) is suggested to be the most plausible origin of the observed spectroscopic feature.

These results confirm that a crystalline 2D form of Si can be grown and stabilized on extended areas of the Ag-passivated Si(111) substrate, provided that the Si atoms are deposited at low flux ($\sim$ 1 ML/hour) on a substrate kept in a narrow temperature range around 200 °C ± 25 °C. In addition, the fact that the initial state S_1 has completely disappeared shows without ambiguity that the segregation of the Ag atoms to reform the initial $\sqrt{3}$-Ag/Si(111) substrate can be discarded at the growth temperature of $\sim$200 °C.

AKNOWLEDGEMENTS

L.G. wishes to thank E. Salomon for fruitful discussion.

[1] G. R. Bhimanapati, Z. Lin, V. Meunier, Y. Jung, J. Cha, S. Das, D. Xiao, Y. Son, M. S. Strano, V. R. Cooper, et al., ACS Nano **9**, 11509 (2015).

[2] J. Zhao, H. Liu, Z. Yu, R. Quhe, S. Zhou, Y. Wang, C. C. Liu, H. Zhong, N. Han, J. Lu, et al., Progress in Materials Science **83**, 24 (2016).

[3] N. Takagi, C.-L. Lin, K. Kawahara, E. Minamitani, N. Tsukahara, M. Kawai, and R. Arafune, Progress in Surface Science **90**, 1 (2015).

[4] A. Kara, H. Enriquez, A. P. Seitsonen, L. L. Y. Voon, S. Vizzini, B. Aufray, and H. Oughaddou, Surface Science Reports **67**, 1 (2012).

[5] K. Quertite, H. Enriquez, N. Trcera, Y. Tong, A. Bendounan, A. J. Mayne, G. Dujardin, P. Lagarde, A. El kenz, A. Benyoussef, et al., Advanced Functional Materials p. 2007013 (2019).

[6] C.-C. Liu, W. Feng, and Y. Yao, Physical Review Letters **107**, 076802 (2011).

[7] L. Meng, Y. Wang, L. Zhang, S. Du, R. Wu, L. Li, Y. Zhang, G. Li, H. Zhou, W. A. Hofer, et al., Nano Letters **13**, 685 (2013).

[8] P. Moras and I. Matsuda, in Monatomic Two-Dimensional Layers (Elsevier, 2019), pp. 113–157.

[9] C. Grazianetti, E. Cinquanta, L. Tao, P. D. Padova, C. Quaresima, C. Ottaviani, D. Akinwande, and A. Molle, ACS Nano **11**, 3376 (2017).

[10] A. Molle, C. Grazianetti, L. Tao, D. Taneja, M. H. Alam, and D. Akinwande, Chemical Society Reviews **47**, 6370 (2018).

[11] T. G. Gill, A. Fleurence, B. Warner, H. Prüser, R. Friedlein, J. T. Sadowski, C. F. Hirjibehedin, and Y. Yamada-Takamura, 2D Materials **4**, 021015 (2017).

[12] R. Friedlein and Y. Yamada-Takamura, Journal of Physics: Condensed Matter **27**, 203201 (2015).

[13] S. Sadeddine, H. Enriquez, A. Bendounan, P. K. Das, I. Vobornik, A. Kara, A. J. Mayne, F. Sirotti, G. Dujardin, and H. Oughaddou, Scientific Reports **7**, 44400 (2017).

[14] D. Chiappe, E. Scalise, E. Cinquanta, C. Grazianetti, B. van den Broek, M. Fanciulli, M. Houssa, and A. Molle, Advanced Materials **26**, 2096 (2013).

[15] R. Pawlak, C. Drechsel, P. D'Astolfo, M. Kisiel, E. Meyer, and J. I. Cerda, Proceedings of the National Academy of Sciences **117**, 228 (2019).

[16] R. Arafune, C.-L. Lin, K. Kawahara, N. Tsukahara, E. Minamitani, Y. Kim, N. Takagi, and M. Kawai, Surface Science **608**, 297 (2013).

[17] A. J. Mannix, B. Kiraly, B. L. Fisher, M. C. Hersam, and N. P. Guisinger, ACS Nano **8**, 7538 (2014).

[18] J. Sone, T. Yamagami, Y. Aoki, K. Nakatsuji, and H. Hirayama, New Journal of Physics **16**, 095004 (2014).

[19] P. Vogt, P. D. Padova, C. Quaresima, J. Avila, E. Frantzeskakis, M. C. Asensio, A. Resta, B. Ealet, and G. L. Lay, Physical Review Letters **108**, 155501 (2012).

[20] C.-L. Lin, R. Arafune, K. Kawahara, M. Kanno, N. Tsukahara, E. Minamitani, Y. Kim, M. Kawai, and N. Takagi, Physical Review Letters **110**, 076801 (2013).

[21] S. K. Mahatha, P. Moras, V. Bellini, P. M. Sheverdyaeva, C. Struzzi, L. Petaccia, and C. Carbone, Physical Review B **89**, 201416 (2014).

[22] S. K. Mahatha, P. Moras, P. M. Sheverdyaeva, R. Flammini, K. Horn, and C. Carbone, Physical Review B **92**, 245127 (2015).

[23] B. Feng, H. Zhou, Y. Feng, H. Liu, S. He, I. Matsuda, L. Chen, E. F. Schwier, K. Shimada, S. Meng, et al., Physical Review Letters **122**, 196801 (2019).

[24] J.-I. Iwata, Y. ichiro Matsushita, H. Nishi, Z.-X. Guo, and A. Oshiyama, Physical Review B **96**, 235442 (2017).

[25] C. Lian and S. Meng, Physical Review B **95**, 245409 (2017).

[26] M. Chen and M. Weinert, Physical Review B **98**, 245421 (2018).

[27] N. W. Johnson, D. Muir, E. Z. Kurmaev, and A. Moewes, Advanced Functional Materials **25**, 4083 (2015).

[28] P. D. Padova, A. Generosi, B. Paci, C. Ottaviani, C. Quaresima, B. Olivieri, E. Salomon, T. Angot, and G. L. Lay, 2D Materials **3**, 031011 (2016).

[29] E. Salomon, R. E. Ajjouri, G. L. Lay, and T. Angot, Journal of Physics: Condensed Matter **26**, 185003 (2014).

[30] T. Shirai, T. Shirasawa, T. Hirahara, N. Fukui, T. Takahashi, and S. Hasegawa, Physical Review B **89**, 241403 (2014).

[31] K. Kawahara, T. Shirasawa, C.-L. Lin, R. Nagao, N. Tsukahara, T. Takahashi, R. Arafune, M. Kawai, and N. Takagi, Surface Science **651**, 70 (2016).

[32] A. Curcella, R. Bernard, Y. Borensztein, M. Lazzeri, A. Resta, Y. Garreau, and G. Prevot, 2D Materials **4**, 025067 (2017).

[33] Y. Borensztein, A. Curcella, S. Royer, and G. Prévot, Physical Review B **92**, 155407 (2015).

[34] P. De Padova, H. Feng, J. Zhuang, Z. Li, A. Generosi, B. Paci, C. Ottaviani, C. Quaresima, B. Olivieri, M. Krawiec, et al., The Journal of Physical Chemistry C **121**, 27182 (2017).

[35] S. Hasegawa, X. Tong, S. Takeda, N. Sato, and T. Nagao, Progress in Surface Science **60**, 89 (1999).

[36] H. Aizawa, M. Tsukada, N. Sato, and S. Hasegawa, Surface Science **429**, L509 (1999).

[37] I. Matsuda, H. Morikawa, C. Liu, S. Ohuchi, S. Hasegawa, T. Okuda, T. Kinoshita, C. Ottaviani, A. Cricenti, M. D'angelo, et al., Physical Review B **68**, 085407 (2003).

[38] H. M. Zhang and R. I. G. Uhrberg, Physical Review B **74**, 195329 (2006).

[39] Y.-X. Yao, X. Liu, Q. Fu, W.-X. Li, D.-L. Tan, and X.-H. Bao, ChemPhysChem **9**, 975 (2008).

[40] P. De Padova, A. Generosi, B. Paci, C. Ottaviani, C. Quaresima, B. Olivieri, M. Kopciuszyński, L. Żurawek, R. Zdyb, and M. Krawiec, Materials **12**, 2258 (2019).

[41] V. Langlais, H. Belkhir, J.-M. Themlin, J.-M. Debever, L.-M. Yu, and P. A. Thiry, Physical Review B **52**, 12095 (1995).

[42] J. Viernow, M. Henzler, W. L. O'Brien, F. K. Men, F. M. Leibsle, D. Y. Petrovykh, J. L. Lin, and F. J. Himpsel, Physical Review B **57**, 2321 (1998).

[43] L. S. O. Johansson, E. Landemark, C. J. Karlsson, and R. I. G. Uhrberg, Physical Review Letters **63**, 2092 (1989).

[44] J. N. Crain, M. C. Gallagher, J. L. McChesney, M. Bissen, and F. J. Himpsel, Physical Review B **72**, 045312 (2005).

[45] I. Matsuda, T. Hirahara, M. Konishi, C. Liu, H. Morikawa, M. D'angelo, S. Hasegawa, T. Okuda, and T. Kinoshita, Physical Review B **71**, 235315 (2005).

[46] T. Hirahara, I. Matsuda, M. Ueno, and S. Hasegawa, Surface Science **563**, 191 (2004).

[47] N. Sato, S. Takeda, T. Nagao, and S. Hasegawa, Physical Review B **59**, 2035 (1999).

[48] J. N. Crain, K. N. Altmann, C. Bromberger, and F. J.

Himpsel, Physical Review B **66**, 205302 (2002).
[49] H. Jeong, H. W. Yeom, and S. Jeong, Physical Review B **77**, 235425 (2008).
[50] J. A. Theobald, N. S. Oxtoby, M. A. Phillips, N. R. Champness, and P. H. Beton, Nature **424**, 1029 (2003).
[51] S. Ohno, H. Tanaka, K. Tanaka, K. Takahashi, and M. Tanaka, Physical Chemistry Chemical Physics **20**, 1114 (2018).
[52] E. Annese, A. Rosi, J. Fujii, and K. Sakamoto, The Journal of Physical Chemistry C **119**, 20065 (2015).
[53] H. M. Zhang, K. Sakamoto, and R. I. G. Uhrberg, Physical Review B **70**, 245301 (2004).
[54] P. M. Sheverdyaeva, S. K. Mahatha, P. Moras, L. Petaccia, G. Fratesi, G. Onida, and C. Carbone, ACS Nano **11**, 975 (2017).
[55] T. Yamagami, J. Sone, K. Nakatsuji, and H. Hirayama, Applied Physics Letters **105**, 151603 (2014).
[56] S. Mahatha, P. Moras, P. Sheverdyaeva, V. Bellini, T. Menteş, A. Locatelli, R. Flammini, K. Horn, and C. Carbone, Journal of Electron Spectroscopy and Related Phenomena **219**, 2 (2017).
[57] W. C. Fan, A. Ignatiev, H. Huang, and S. Y. Tong, Physical Review Letters **62**, 1516 (1989).
[58] F. Ancilotto, A. Selloni, and E. Tosatti, Physical Review B **43**, 14726 (1991).
[59] P. Kocán, O. Krejčí, and H. Tochihara, Journal of Vacuum Science & Technology A: Vacuum, Surfaces, and Films **33**, 021408 (2015).
[60] J. Chen, Y. Du, Z. Li, W. Li, B. Feng, J. Qiu, P. Cheng, S. X. Dou, L. Chen, and K. Wu, Scientific Reports **5**, 13590 (2015).
[61] Z.-X. Guo, S. Furuya, J. ichi Iwata, and A. Oshiyama, Physical Review B **87**, 235435 (2013).
[62] S. Cahangirov, M. Audiffred, P. Tang, A. Iacomino, W. Duan, G. Merino, and A. Rubio, Physical Review B **88**, 035432 (2013).
[63] It is known that the Ag adatoms transfer charge into the surface state thus reducing the band bending [35].
[64] The silicene lattice is, within the present energy and k resolutions, virtually the same as that of the last two atomic planes of Si(111).